



Selective conversion of aqueous glucose to value-added sugar aldose on TiO₂-based photocatalysts



Ruifeng Chong, Jun Li, Yi Ma, Bao Zhang, Hongxian Han, Can Li*

State Key Laboratory of Catalysis, Dalian Institute of Chemical Physics, Chinese Academy of Sciences, Dalian National Laboratory for Clean Energy, 457 Zhongshan Road, Dalian 116023, China

ARTICLE INFO

Article history:

Received 23 December 2013

Revised 25 February 2014

Accepted 18 March 2014

Keywords:

Photocatalysis

Biomass

Glucose

Reactive oxygen species

TiO₂

ABSTRACT

We describe here a photocatalytic process for direct conversion of glucose to value-added chemicals (arabinose and erythrose) and H₂ in water under mild reaction conditions without additional acid or base. The total selectivity for the production of arabinose and erythrose on rutile TiO₂-based photocatalyst reaches 91% at 65% conversion. More importantly, it has been demonstrated for the first time that the photodegradation of glucose initially involves C1–C2 bond cleavage (α -scission) to produce arabinose in the presence of water as solvent. To unravel the high selectivity on rutile TiO₂, EPR and glucose reaction were carried out on rutile TiO₂ in the presence of H₂O₂. It was found that the selectivity of the products is mainly dependent on the reactive oxygen species: the hydroxyl radicals (\cdot OH) may lead to low selectivity, while the peroxy species lead to a high selectivity. The advantages of the photocatalytic approach for conversion of biomass to value-added chemicals include (1) operation at low reaction temperature, (2) benign environmental effects due to using only water as both solvent and oxidant precursor, and (3) being wasteless due to high selectivity with H₂ as the by-product.

© 2014 Elsevier Inc. All rights reserved.

1. Introduction

Glucose is one of the main products of photosynthesis found in plants. It is the most abundant and cheapest monosaccharide in nature among the hexose sugars (such as glucose, fructose, and galactose), which can be directly obtained by hydrolysis of polysaccharides such as starch and cellulose. Biochemical processes of fermentation dominate the field of the use of glucose, because of their high selectivity and productivity under mild reaction conditions. Lactic acid [1], succinic acid [2], and gluconic acid [3] can be obtained by glucose fermentation processes in industry. On the other hand, chemical catalysis processes often give much higher productivity with reduced costs related to the large-scale product work-up. Nowadays, some important industrial and pharmaceutical chemicals, such as sorbitol [4,5], 5-hydroxymethylfurfural (HMF) [6–8], and lactic acid [9,10], are produced by catalytic processing of glucose. Though these two processes largely satisfy current industrial needs, the future application of glucose will largely depend on the costs of products. An alternative method for the conversion of glucose is in high demand.

Photocatalysis as an innovative approach has attracted much attention to H₂ production [11,12] and organic reactions [13,14] under mild reaction conditions. It might be an ideal approach for the conversion of glucose to value-added chemicals. With the depletion of fossil fuels, it is highly desirable to use abundant solar energy as the energy source to produce so-called “solar fuels” such as H₂ by water splitting or biomass conversion, or to do “green” chemistry to produce value-added chemicals by photocatalytic conversion of biomass under mild reaction conditions. TiO₂ has often been selected as a model photocatalyst for the study of biomass reforming, because it has a negative potential of the conduction band for H₂ production and a sufficiently positive potential of the valence band for biomass oxidation. Many advances have been achieved in H₂ production from glucose on TiO₂ photocatalyst [11,12]. Recently, it was reported that photocatalytic oxidation of glucose on nanostructured TiO₂ can produce glucaric acid, gluconic acid, and arabitol [15]. The products’ selectivity varies in the ratio of CH₃CN/H₂O. The best total selectivity could be up to 71.3% at 11% glucose conversion under optimized experimental conditions. However, the total selectivity was zero when water was used as the sole solvent. Thus, the low selectivity is still an obstacle for photocatalytic conversion of glucose, especially when water is used as the solvent [16,17]. Aiming at promoting green chemistry processes for biomass conversion and considering the solubility of glucose, water should be an ideal reaction medium for glucose

* Corresponding author. Fax: +86 411 84694447.

E-mail address: canli@dicp.ac.cn (C. Li).

conversion to value-added chemicals. We believe that the selectivity of glucose conversion in water can be solved by better understanding its conversion mechanism and tailoring the design of efficient photocatalysts accordingly.

In this work, the photocatalytic reactions of glucose conversion were performed on TiO₂-based photocatalysts dispersed in water under anaerobic conditions without adding any acid or base. The major products were arabinose and erythrose formed by α -scission of glucose, together with H₂ and HCOOH as by-products (Scheme 1). Importantly, on rutile TiO₂-based photocatalyst, the total selectivity for arabinose and erythrose can be up to 91% at 65% conversion. The behavior of α -scission was also observed for arabinose and erythrose during the reactions, indicating that it is a common feature of sugar aldose degradation. Further investigation reveals that the behavior of α -scission is mainly determined by the type of aldehyde group of sugar aldose and the oxidative intermediate species derived from water oxidation during photocatalysis. It should be noted here that arabinose, which is traditionally prepared by oxidative degradation of gluconic acid or its derivatives, is an important precursor for the production of vitamin B2, DNA, arabinosine, etc. [18,19]. Hydrolysis of erythrose under mild conditions can give erythritol, a natural polyol sweetener for the replacement of sugar due to its low calorie level [20]. To the best of our knowledge, this is the first report of the photocatalytic selective conversion of glucose to value-added chemicals with water as the sole oxidant and solvent under mild reaction conditions. It demonstrates that “green” photocatalytic processes would be a competitive approach for the reforming of cheap and abundant biomass feedstocks into value-added chemicals.

2. Experimental section

2.1. Preparation of catalysts

TiO₂ samples were synthesized by a modified hydrothermal method reported in the literature [21]. The desired volumes (1 mL and 6 mL for the synthesis of anatase and rutile, respectively) of HCl (36.5%, Shanghai Guoyao) were dropped into 15 mL of titanium isopropoxide (97%, Alfa Aesar) in a 100-mL Teflon-lined autoclave at room temperature and then kept at 453 K for 36 h. After the autoclave was cooled to room temperature, the resulting white precipitates were filtered out and washed sequentially with 5 mol L⁻¹ NaOH solution and distilled water until the pH of the filtrate was neutral. The final products were dried in an oven at 353 K overnight. Commercial P25 (Degussa) was used as reference.

Co-catalysts of 0.2 wt% Rh (or Pt, Pd) or 1.0 wt% Cu, Ni were loaded onto TiO₂ at the very beginning of the reaction by an in situ photodeposition method using the corresponding precursor RhCl₃ (or H₂PtCl₆·6H₂O, PdCl₂, CuCl₂, or Ni(NO₃)₂) in aqueous solution.

2.2. Typical conditions for glucose conversion reaction

Photocatalytic reactions were carried out at 288 K in a Pyrex reaction cell connected to a closed gas circulation and vacuum system. A 300 W top-irradiated xenon lamp was used as a light source. Prior to illumination, the system was deaerated by evacuation. Typically, 0.1 g of catalyst was suspended in a 100 mL glucose solution (0.0125 mol L⁻¹).

The conversion and selectivity for the glucose conversion are defined as follows:

$$\text{Conversion} = (c_{r0} - c_r) / c_{r0} \cdot 100\%;$$

$$\text{Selectivity} = c_p / (c_{r0} - c_r) \cdot 100\%;$$

$$\sum_{\text{Sel.}} = \text{Selectivity}_{\text{arabinose}} + \text{Selectivity}_{\text{erythrose}}.$$

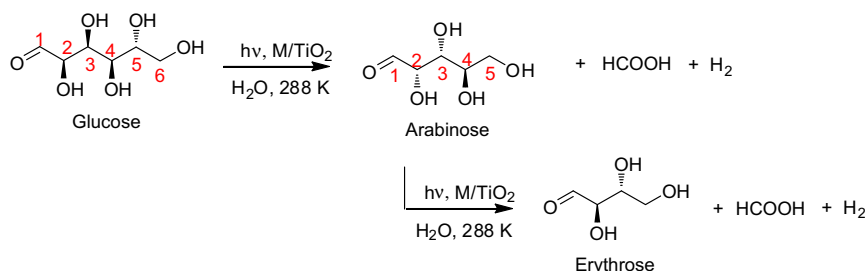
c_{r0} and c_r represent for the initial and final concentration of the reactant, respectively, and c_p stands for the concentration of the product.

2.3. Characterization

The phase compositions in the bulk and surface regions of TiO₂ were characterized using XRD and visible Raman spectroscopy. XRD patterns were obtained on a Rigaku MiniFlex diffractometer with a CuK α radiation source. Diffraction patterns were collected from 20° to 80° at a speed of 5° min⁻¹. Visible Raman spectra were recorded on a Jobin–Yvon U1000 scanning double monochromator with a spectral resolution of 4 cm⁻¹. The line at 532 nm from a DPSS 532 Model 200 532 nm single-frequency laser was used as the excitation source. The morphology was examined with a QUANTA 200F SEM. TEM images were obtained using a Tecnai G² Spirit (FEI Company) at an acceleration voltage of 120 kV. HRTEM images were obtained on a Tecnai G² F30 S-Twin (FEI Company) with an acceleration voltage of 300 kV. The BET surface area of the samples was measured based on nitrogen adsorption at 77 K using a Micromeritics ASAP 2000 adsorption analyzer.

The qualitative analysis was performed by ultra-high-performance liquid chromatography–single-quadrupole mass spectrometry (UPLC/Q-TOF micro, Waters, USA). An Alltech OA-1000 column was used for the sample separation with a flow rate of 0.35 mL min⁻¹ and column temperature at room temperature. Water was used as the mobile phase. MS was operated in negative ESI mode.

Mass spectrometry analyses were conducted using a MALDI TOF-TOF 5800 analyzer (AB SCIEX, Shanghai, China) equipped with a neodymium: yttrium–aluminum–garnet laser (laser wavelength 349 nm) in reflection positive-ion mode. Portions of 2 μ L of the standard sample mixture (glucose, arabinose, erythrose, and glyceraldehyde) and the reaction solution were mixed with 2 μ L of



Scheme 1. Conversion of aqueous glucose with M/TiO₂ by photocatalysis.

the matrix (α -cyano-4-hydroxycinnamic acid (CHCA) in water) before spotting on the target plate.

The gaseous products were analyzed by online gas chromatography (GC) with a TDX-01 column. The amount of hydrogen produced was measured by a thermal conductivity detector, and CO_2 was detected by a flame ionization detector after it was converted into CH_4 in a methanator.

The liquid products quantitative analysis was carried out using HPLC (Agilent 1200) with a refractive index (RI) ultraviolet (UV) detector for glucose, arabinose, erythrose, and formic acid. Reactant and products were separated on an ion exclusion column (Alltech OA-1000) heated to 333 K. The eluent was a solution of H_2SO_4 (0.005 mol L^{-1}), the flow was 0.35 mL min^{-1} , and the temperature for RI was 328 K. Products were identified by comparison with standard samples. Glucose (>99.5%), arabinose, erythrose, formic acid, and gluconic acid were obtained from Sigma-Aldrich.

The radical intermediates formed during the photocatalytic courses were probed by trapping with 5,5-dimethyl-1-pyrroline *N*-oxide (DMPO) and identified using electron paramagnetic resonance (EPR) spectra recorded on a Bruker EPR A200 spectrometer. The samples containing 1 mg mL^{-1} $\text{TiO}_2\text{-R}$ and 0.05 mol L^{-1} DMPO were vacuumized and ventilated with argon. After that, the samples were introduced into a homemade EPR quartz tube inside the microwave cavity and illuminated with a 300-W xenon lamp (CERAMAX LX-300). For comparison, all of the EPR spectra were recorded under the same experimental conditions with the following EPR parameter settings: microwave frequency, 9.40 GHz; center field, 3360 G; sweep width, 100 G; modulation frequency, 100 kHz; and power, 20.00 mW.

3. Results and discussion

3.1. The phase structure and morphology of TiO_2 samples

The XRD patterns mainly provide the crystallinity information for the bulk TiO_2 . As shown in Fig. 1A, the $\text{TiO}_2\text{-A}$ sample shows Bragg diffraction peaks with 2θ at 25.6° , 38.1° , 48.3° , 54.2° , and 55.3° , which represent the indices of the (101), (004), (200), (105), and (211) planes (JCPDS 21-1272), while the $\text{TiO}_2\text{-R}$ sample shows strong diffraction peaks with 2θ at 27.7° , 36.3° , 41.5° , and 54.6° , which correspond to the indices of the (110), (101), (111), and (211) planes (JCPDS 21-1276) of the rutile phase. The XRD patterns show that the obtained $\text{TiO}_2\text{-A}$ and $\text{TiO}_2\text{-R}$ samples are in highly pure anatase and rutile phases in bulk, respectively. Visible Raman is a surface-sensitive technique that can be used effectively to characterize the surface properties of a material. Fig. 1B shows the visible Raman spectra of the prepared TiO_2

samples. The strong Raman bands at 143, 191, 395, 515, and 638 cm^{-1} suggest that the sample $\text{TiO}_2\text{-A}$ is mainly in the anatase phase. The Raman bands at 235, 445, and 612 cm^{-1} for sample $\text{TiO}_2\text{-R}$ are the characteristic bands of rutile phase TiO_2 with no observation of the other impurity. Raman peaks for these two samples indicate that the surface compositions of the obtained $\text{TiO}_2\text{-A}$ and $\text{TiO}_2\text{-R}$ are also highly pure anatase and rutile phase TiO_2 , respectively. The reference P25 is a standard material in the field of photocatalytic reactions, which contains anatase and rutile phases at a ratio of about 3: 1.

The morphologies and dimensions of the prepared TiO_2 samples were studied by SEM and TEM. Fig. 2A and C are the SEM and TEM images of $\text{TiO}_2\text{-A}$, respectively. It can be seen that $\text{TiO}_2\text{-A}$ is composed of aggregated nanoparticles with size ca. 9 nm, while $\text{TiO}_2\text{-R}$ shows a rodlike shape with dimensions ca. 50 nm in width and 300 nm in length, as shown in Fig. 2B and D. The specific surface areas of $\text{TiO}_2\text{-A}$, $\text{TiO}_2\text{-R}$, and the commercial P25 reference are 123.4, 25.9, and $58.0 \text{ m}^2 \text{ g}^{-1}$, respectively.

3.2. Photocatalytic conversion of aqueous glucose on TiO_2 -based catalysts

The $\text{TiO}_2\text{-A}$, $\text{TiO}_2\text{-R}$, and P25 samples loaded with various metal co-catalysts were tested for the conversion of aqueous glucose. The photocatalytic reactions were performed under anaerobic conditions at 288 K without additional acid or base. The preliminary results show that no reaction takes place in the absence of light or catalyst. Under the same experimental conditions with the same amount of metal co-catalysts loaded, Rh was found to be the most effective co-catalyst for glucose conversion. Table 1 lists the results of the reaction on Rh/ TiO_2 . It can be seen that the major gaseous products are H_2 and CO_2 , accompanied by CO as minor product. The major liquid products are arabinose, erythrose, formic acid, and gluconic acid, accompanied by glyceraldehydes as a minor product (GA) (see the Supplementary information, Figs. S1–S9).

To compare the intrinsic activity of catalysts, the glucose conversion rates are normalized by the specific surface area of TiO_2 . As shown in Table 2, the order of the activity is $\text{TiO}_2\text{-R} > \text{P25} > \text{TiO}_2\text{-A}$. The activity of $\text{TiO}_2\text{-R}$ was about 14 times that of $\text{TiO}_2\text{-A}$ and 6 times that of P25. The total selectivity for arabinose and erythrose also varied with the different phases of TiO_2 . $\text{TiO}_2\text{-A}$ displayed the lowest total selectivity for arabinose and erythrose but gave the highest CO_2/H_2 molar ratio of 0.48 (the theoretical value is 0.5 if glucose is completely converted into CO_2 and H_2), indicating sufficient C–C cleavage by $\text{TiO}_2\text{-A}$. In contrast, $\text{TiO}_2\text{-R}$ displayed the highest total selectivity of 96% for arabinose and erythrose accompanied by the lowest value of the CO_2/H_2 ratio (0.017), indicating that $\text{TiO}_2\text{-R}$ has a mild ability for the cleavage of C–C bonds. It

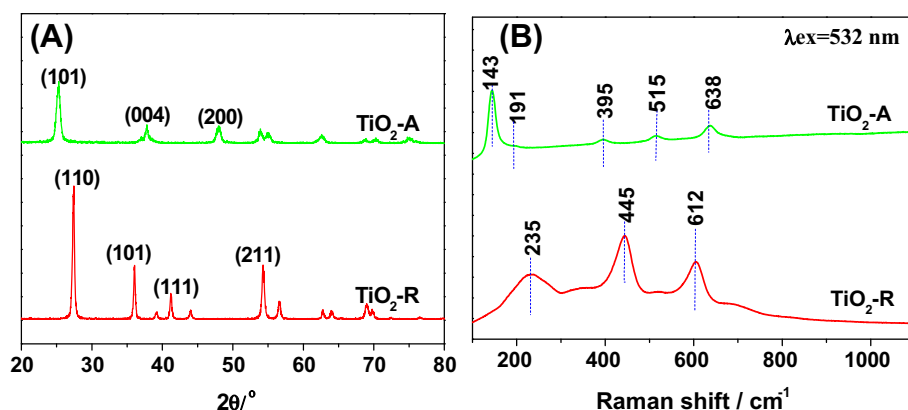


Fig. 1. Typical XRD patterns (A) and visible Raman spectra (B) of the home-prepared TiO_2 .

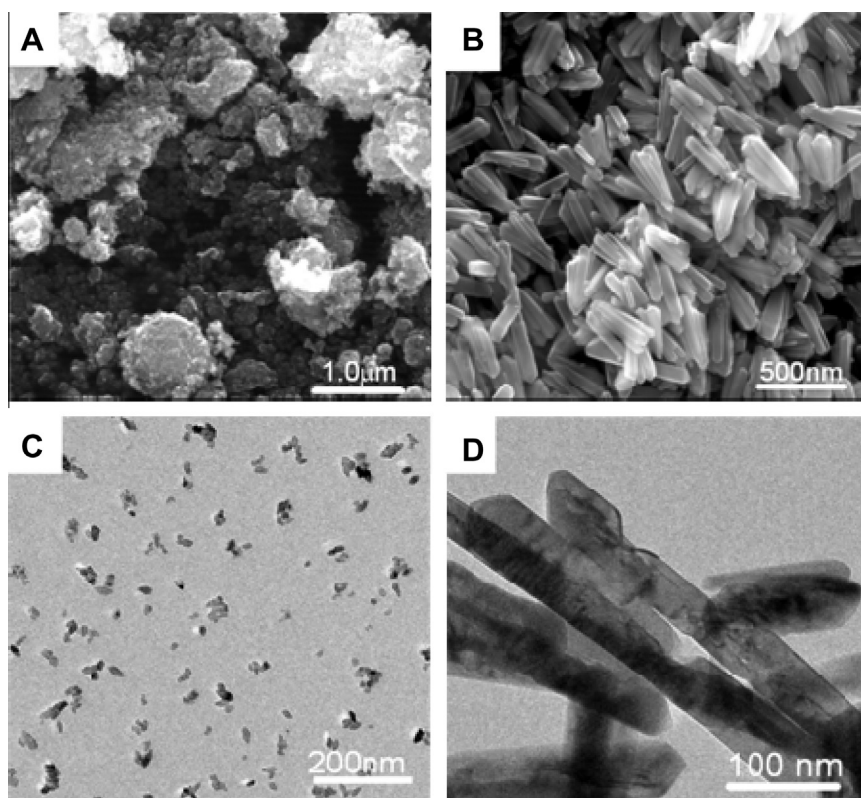


Fig. 2. SEM and TEM images of TiO₂-A (A and C) and TiO₂-R (B and D).

Table 1
The amounts of the products of the photocatalytic conversion of aqueous glucose on Rh/TiO₂ catalysts.

TiO ₂	The amounts of the products (μmol)								Consumed glucose (μmol)
	H ₂	Arabinose	Erythrose	GA	Gluconic acid	HCOOH	CO	CO ₂	
TiO ₂ -A	335	99	9	7	6	81	2.7	160	200
TiO ₂ -R	846	445	121	41	–	632	0.6	15	588
P25	472	132	20	14	21	127	0.6	170	217

Notes: Reaction conditions: catalyst, 0.1 g; co-catalyst, 0.2 wt% Rh; 0.0125 mol L⁻¹ aqueous glucose solution, 100 mL; light source, xenon lamp (300 W); reaction temperature, 288 K; reaction time, 4 h.

Table 2
The selectivity of the products of the photocatalytic conversion of aqueous glucose on Rh/TiO₂ catalysts.

TiO ₂	The activity of glucose (μmol m ⁻²)	Selectivity (%)			Σ _{sel.} (%)	C-balance (%)	CO ₂ /H ₂ ^a
		Arabinose	Erythrose	Gluconic acid			
TiO ₂ -A	16.2	49.4	4.5	3.2	53.9	66.5	0.478
TiO ₂ -R	227.0	74.7	20.6	0	95.3	98.6	0.018
P25	37.4	60.7	9.0	9.6	69.7	86.5	0.359

Note: See Table 1 for the reaction conditions.

^a The complete conversion of glucose to H₂ and CO₂ (C₆H₁₂O₆ + 6H₂O = 12H₂ + 6CO₂) with a molar ratio of CO₂/H₂ is 0.5.

should also be noted that gluconic acid was also produced from aqueous glucose on TiO₂-A and P25 with a selectivity of 3.2% and 9.6%, respectively, but it was not detected on TiO₂-R.

To exclude the influence of metal co-catalysts, several experiments were performed by substituting typical noble and cheap metals (Pt, Pd, Cu, and Ni) for Rh. As shown in Table 3, without co-catalyst loaded on TiO₂-R, the conversion of glucose was significantly enhanced. When co-catalyst was loaded on TiO₂-R, the conversion of glucose was significantly further enhanced. As co-catalyst, Rh shows a higher conversion than that of Pt, and Pd shows a comparable activity to Rh. Cheap metals Cu and Ni also

can be used for conversion of glucose, giving conversions of 41% and 27%, respectively. However, the total selectivity of arabinose and erythrose shows no significant changes with different kinds of co-catalysts. This indicates that the metal co-catalysts can serve as efficient electron traps preventing photogenerated electrons and holes from recombining and as active sites for H₂ production, while they show a negligible influence on the selectivity. The above results suggest that the reaction pathways of glucose photocatalytic conversion are quite different on the different TiO₂-based photocatalysts; especially, the product selectivities are strongly dependent on the phase structure of TiO₂.

Table 3
Photocatalytic conversion of aqueous glucose with different TiO₂-R-loaded co-catalysts.

Co-catalyst	Reaction time (h)	Conversion (%)	Selectivity (%)		$\Sigma_{\text{Sel.}}$ (%)
			Arabinose	Erythrose	
None	4	Trace	–	–	–
Pt	4	35.9	78.6	21.0	99.4
Rh	4	47.0	74.7	20.6	95.3
	6	61.3	68.9	23.6	92.5
Pd	6	59.1	72.3	24.7	97.0
Cu	6	40.7	85.9	12.5	98.4
Ni	6	27.0	88.6	7.5	96.1

Notes: Reaction conditions: catalyst, 0.1 g; co-catalyst, 0.2 wt% Pt, Rh, Pd; 1 wt% Cu, Ni; 0.0125 mol L⁻¹ aqueous glucose solution, 100 mL; light source, xenon amp (300 W); reaction temperature, 288 K.

3.3. The glucose conversion reaction on TiO₂-R catalysts

Fig. 3 shows the results of a representative experimental run carried out on Rh/TiO₂-R. The conversion rates and the selectivities are reported as functions of the irradiation time. The carbon balance was quantified more than 96%. With prolonged irradiation time, the glucose conversion rate increases and the selectivity for arabinose slowly decreases, while that for erythrose gradually increases, indicating that the reaction is a kind of typical tandem reaction. The selectivities for arabinose and erythrose were ca. 67% and 24%, respectively, even when the glucose conversion reached 65%. No detection of C2 product (Table 1) suggests that erythrose did not arise from the C2–C3 bond cleavage. Examination of the amounts of the products and the consumed glucose indicates that glucose reacted nearly stoichiometrically with H₂O on TiO₂-R (Table 1). From these experimental results, it is feasible to assume that the glucose conversion reaction is through α -scission, which might be initiated by some mildly reactive oxygen species generated by water oxidation during photolysis. In other words, water may play the role of both solvent and oxidant precursor.

We further carried out the photocatalytic reactions on TiO₂-R using glucose, arabinose, and erythrose as substrates. As shown in Fig. 4, arabinose is the main product of glucose, erythrose is the main product of arabinose, and glyceraldehyde is the main product of erythrose. This suggests that selective α -scission is a common feature for sugar aldoses in photocatalytic processes on TiO₂-R and further confirms that the photocatalytic conversion of glucose occurs through tandem reaction. The proposed pathway

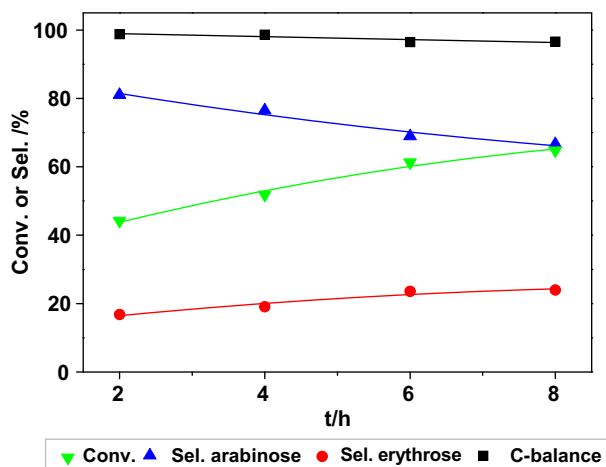


Fig. 3. Experimental results for photocatalytic conversion of aqueous glucose with Rh/TiO₂-R. Reaction conditions: catalyst, 0.1 g; co-catalyst, 0.2 wt% Rh; 0.0125 mol L⁻¹ aqueous glucose solution, 100 mL; light source, xenon lamp (300 W); reaction temperature, 288 K.

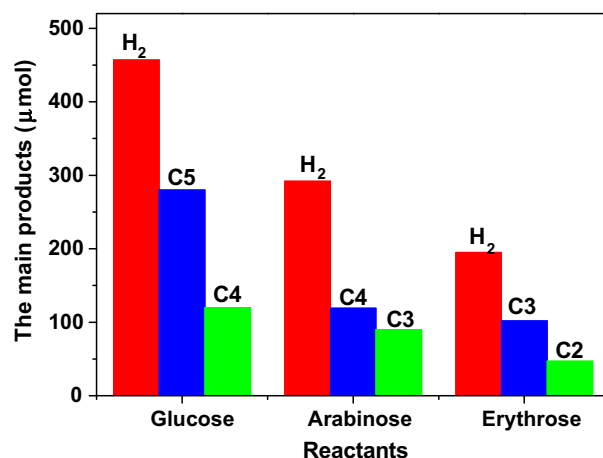


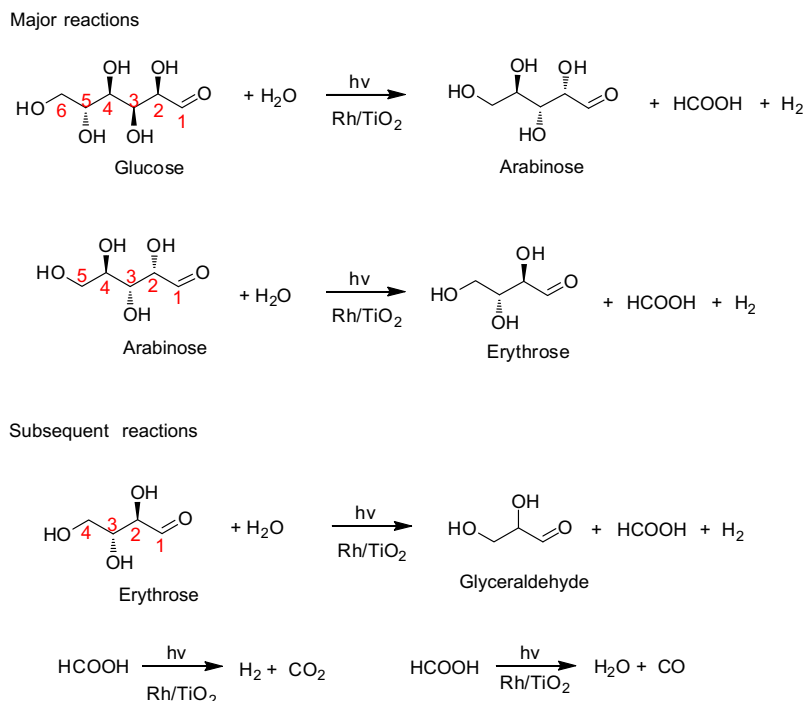
Fig. 4. The initial H₂ production rate from photocatalytic conversion of glucose, arabinose, erythrose solution with Rh/TiO₂-R. Reaction conditions: catalyst, 0.1 g TiO₂-R; co-catalyst, 0.2 wt% Rh; 0.010 mol L⁻¹ aqueous glucose, arabinose, or erythrose solution, 100 mL; light source, xenon lamp (300 W); reaction temperature, 288 K; reaction time, 1 h. The molecules glucose, arabinose, erythrose, glyceraldehydes, and glycolaldehyde are denoted as C6, C5, C4, C3, and C2, respectively.

of the glucose conversion reaction can be summarized as shown in Scheme 2. First, glucose reacts with H₂O through dehydrogenation and a C–C bond cleavage reaction to produce H₂, arabinose, and HCOOH. Then, the accumulated arabinose reacts with H₂O to form erythrose and HCOOH, followed by conversion of erythrose to glyceraldehyde. At the same time, the by-product formic acid may be directly oxidized by holes to give CO₂ and H₂.

3.4. The roles of the reactive oxygen species derived from water

As has been reported, the oxidation of H₂O by photogenerated holes can produce $\cdot\text{OH}$ on the surface of TiO₂-A and peroxy species on TiO₂-R, respectively [22]. The presence of highly active $\cdot\text{OH}$ leads to low selectivity, while the participation of mild active peroxy species in the reaction often gives high selectivity.

An EPR spin-trap technique with DMPO as a radical trap was used to detect the reactive oxygen species. No apparent EPR signal was observed in the absence of TiO₂ when the reaction mixture was UV-illuminated for up to 10 min (see the Supplementary information, Fig. S10). As shown in Fig. 5, in the TiO₂-R/H₂O/DMPO system, a very weak EPR signal assignable to DMPO- $\cdot\text{OH}$ was observed upon UV illumination, which might be produced by the oxidation of the surface hydroxyl of TiO₂-R. With prolonged irradiation time, the signals of DMPO- $\cdot\text{OH}$ disappeared and simultaneously a seven-line paramagnetic signal due to the DMPO oxidized product 5,5-dimethyl-1-pyrrolidone-2-oxyl ($\cdot\text{DMPO-X}$)



Scheme 2. The proposed reaction routes for photocatalytic conversion of aqueous glucose with Rh/TiO₂-R.

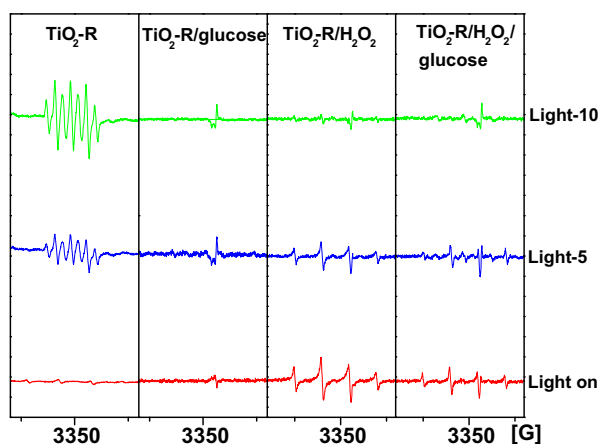


Fig. 5. Typical EPR spectra for the reactive species generated from TiO₂-R suspension in argon under light illumination, in the presence of the spin-trap DMPO. Concentrations: TiO₂, 1 mg mL⁻¹; DMPO, 0.05 mol L⁻¹. The signals obtained upon irradiating are denoted as Light on, those after irradiating for 5 min are denoted as Light-5', and similarly, those after irradiating for 10 min as Light-10.

evolved. The oxidation of DMPO molecules to [•]DMPO-X (see the [Supplementary information, Reaction S1](#)) in different oxidative environments was monitored previously, and the corresponding appropriate reaction pathways were proposed [23,24]. Similarly, the oxidation of DMPO to [•]DMPO-X in this work also reflects the produced reactive oxygen species upon irradiation. Under anaerobic conditions, the reactive oxygen species can only be generated from the oxidation of H₂O by photogenerated holes. According to the literature, the photooxidation of water on rutile TiO₂ is initiated by a nucleophilic attack of a H₂O molecule on a surface-trapped hole at a lattice O site (Ti-O[•]), forming surface peroxy species, TiOOH [25,26]. Therefore, it can be inferred that the peroxy species is the reactive oxygen species from water on TiO₂-R.

Furthermore, to gain more insight into the effect of the reactive oxygen species on the product selectivities, EPR control

experiments using H₂O₂ as the [•]OH radical precursor were performed. When H₂O₂ was added to the TiO₂-R/H₂O/DMPO system, the typical seven-line EPR signal disappeared, and the four characteristic peaks due to DMPO-[•]OH appeared. The generated [•]OH radicals are mainly from the decomposition of H₂O₂ (H₂O₂ + TiO₂ (e) → [•]OH + OH⁻). It should also be noted that the intensity of the DMPO-[•]OH EPR signal decreased upon continuous irradiation. This phenomenon can be explained as the multiaddition of hydroxyl radicals to DMPO, resulting either in the generation of EPR-silent products or in the decomposition of the spin-trapped adduct [27]. Subsequently, when glucose was introduced into the H₂O/DMPO/TiO₂-R/H₂O₂ system, the EPR signal became weak, indicating that [•]OH generated from H₂O₂ could react rapidly with glucose.

For comparison, the experiment of photocatalytic conversion of glucose on TiO₂-R was also carried out in the presence of H₂O₂. As shown in [Table 4](#), the total selectivity was decreased to 43%, which is lower than that without H₂O₂. This result further confirms that the C-C bond of glucose is overcleaved by [•]OH. In contrast, the mild peroxy species generated on TiO₂-R can partially cleave the C-C bond of glucose [28].

3.5. The effect of the aldehyde group of glucose on C-C bond cleavage

To explore whether the reaction pathway is unique for sugar aldoses on TiO₂-R, the photocatalytic reactions of polyols (such

Table 4
Photocatalytic conversion of aqueous glucose with Rh/TiO₂-R in the presence of H₂O₂.

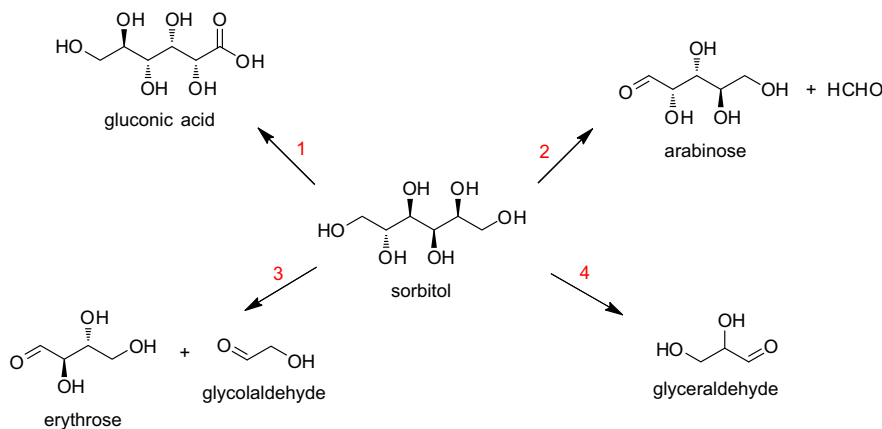
H ₂ O ₂ (mol L ⁻¹)	Conversion (%)	Selectivity (%)		Σ _{sel.} (%)
		Arabinose	Erythrose	
0	47.0	74.7	20.6	95.3
0.02	38.8	21.1	22.2	43.3

Notes: Reaction conditions: catalyst, 0.1 g; co-catalyst, 0.2 wt% Rh; 0.0125 mol L⁻¹ aqueous glucose solution, 100 mL; light source, xenon lamp (300 W); reaction temperature, 288 K; reaction time, 4 h.

Table 5
Photocatalytic conversion of aqueous sorbitol with TiO₂-R.

Time (h)	Consumed sorbitol (mmol L ⁻¹)	Main products (mmol L ⁻¹)							
		Gluconic acid C6	Pentose C5	Erythrose C4	Glyceraldehyde C3	Glycolaldehyde C2	HCHO C1	HCOOH C1	CO ₂ C1
2	9.30	0.93	1.72	2.02	2.36	4.58	4.07	2.57	0.33
4	13.76	1.05	2.09	2.79	3.38	7.55	6.43	5.61	0.82

Notes: Reaction conditions: catalyst, 0.1 g; co-catalyst, 0.2 wt% Rh; 0.02 mol L⁻¹ aqueous sorbitol solution, 100 mL; light source, xenon lamp (300 W); reaction temperature, 288 K.



Scheme 3. The possible reaction routes for photocatalytic conversion of aqueous sorbitol with Rh/TiO₂-R.

as sorbitol) were also performed under identical experimental conditions. As shown in Table 5, the products C6, C5, C4, C3, C2, and C1 were formed from sorbitol and the amounts of the products were increased with prolonged reaction time. This indicates that four reaction pathways coexist in the reaction of sorbitol, including oxidation of the terminal hydroxyl and three types of C–C bond cleavage (C1–C2, C2–C3, C3–C4) (Scheme 3). Other polyols show reaction pathways similar to that of sorbitol (see the Supplementary information, Table S1). Taken together, these results demonstrate that the reaction pathways of sugar aldose and polyols on TiO₂-R are different from those on TiO₂-A. Our experimental results show that α -scission is codetermined by the aldehyde group of sugar aldose and the peroxy species generated on TiO₂-R.

4. Conclusion

We have succeeded in photocatalytic conversion of aqueous glucose to value-added chemicals arabinose and erythrose with H₂ as by-product using a TiO₂-based photocatalyst under mild conditions. The total selectivity of arabinose and erythrose was more than 91% at 65% conversion of glucose on TiO₂-R. In this process, water plays the roles of oxidant precursor and solvent, and the reactive oxygen species derived from water determines the selectivity of products. The reaction occurs mainly through α -scission by TiO₂-R, which is a characteristic pathway of sugar aldose degradation. Our work provides a feasible process for conversion of carbohydrates to value-added chemicals and H₂.

Acknowledgments

This work was financially supported by the National Natural Science Foundation of China (NSFC Grant 21090340/21090341, 21061140361) and the Ministry of Science and Technology of China (MOST Grant 2014CB239400).

Appendix A. Supplementary material

Supplementary data associated with this article can be found, in the online version, at <http://dx.doi.org/10.1016/j.jcat.2014.03.009>.

References

- [1] M.A. Patel, M.S. Ou, R. Harbrucker, H.C. Aldrich, M.L. Buszko, L.O. Ingram, K.T. Shanmugam, A.K.T.S. Lonnie, O. Ingram, *Appl. Environ. Microbiol.* 72 (2006) 3228–3235.
- [2] Y. Liu, P. Zheng, Z. Sun, Y. Ni, J. Dong, P. Wei, J. Chem. Technol. Biotechnol. 83 (2008) 722–729.
- [3] E.J. Tomotani, L.C.M.D. Neves, M. Vitolo, *Appl. Biochem. Biotechnol.* 121–124 (2005) 149–162.
- [4] H. Li, W.J. Wang, J.F. Deng, *J. Catal.* 191 (2000) 257–560.
- [5] E. Crezee, B.W. Hoffer, R.J. Berger, M. Makkee, F. Kapteijn, J.A. Moulijn, *Appl. Catal. A* 251 (2003) 1–17.
- [6] G. Yong, Y. Zhang, J.Y. Ying, *Angew. Chem. Int. Ed.* 47 (2008) 9345–9348.
- [7] Y.J. Pagán-Torres, T. Wang, J.M.R. Gallo, B.H. Shanks, J.A. Dumesic, *ACS Catal.* 2 (2012) 930–934.
- [8] H. Zhao, J.E. Holladay, H. Brown, Z.C. Zhang, *Science* 316 (2007) 1597–1600.
- [9] M.S. Holm, S. Saravanamurugan, E. Taarning, M.A. Abdel-Rahman, *Science* 328 (2010) 602–605.
- [10] G. Epiane, J.C. Laguerre, A. Wadouachi, D. Marek, *Green Chem.* 12 (2010) 502–506.
- [11] J. Zhang, Q. Xu, Z. Feng, M. Li, C. Li, *Angew. Chem. Int. Ed.* 47 (2008) 1766–1769.
- [12] X. Fu, J. Long, X. Wang, D.Y.C. Leung, Z. Ding, L. Wu, Z. Zhang, Z. Li, X. Fu, *Int. J. Hydrogen Energy* 33 (2008) 6484–6491.
- [13] G. Palmisano, E. García-López, G. Marci, V. Loddo, S. Yurdakal, V. Augugliaro, L. Palmisano, *Chem. Commun.* 46 (2010) 7074–7089.
- [14] V. Augugliaro, M. Bellardita, V. Loddo, G. Palmisano, L. Palmisano, S. Yurdakal, *J. Photochem. Photobiol. C: Photochem. Rev.* 13 (2012) 224–245.
- [15] J. Colmenares, A. Magdziarz, A. Bielejewska, *Bioresour. Technol.* 102 (2011) 11254–11257.
- [16] M. Hoffmann, S. Martin, W. Choi, D. Bahnemann, *Chem. Rev.* 95 (1995) 69–96.
- [17] S. Yurdakal, G. Palmisano, V. Loddo, V. Augugliaro, L. Palmisano, *J. Am. Chem. Soc.* 130 (2008) 1568–1569.
- [18] C. Chou, T. Chou, *J. Appl. Electrochem.* 33 (2003) 741–745.
- [19] M. Borovcova, V. Jiricny, V. Stanek, *Method of Production of D-arabinose*, U.S. Patent 4950366 A, 1990.
- [20] J. Stapley, J. Genders, D. Atherton, P. Kendall, *Methods for the Electrolytic Production of Erythrose or Erythritol*, U.S. Patent 7955489 B2, 2006.
- [21] T. Phan, H. Pham, T. Cuong, E. Kim, S. Kim, E. Shin, *J. Cryst. Growth* 312 (2009) 79–85.

- [22] R. Chong, J. Li, X. Zhou, Y. Ma, J. Yang, L. Huang, H. Han, F. Zhang, C. Li, *Chem. Commun.* 50 (2014) 165–167.
- [23] J. Ueda, K. Takeshita, S. Matsumoto, K. Yazaki, M. Kawaguchi, T. Ozawa, *Photochem. Photobiol.* 77 (2003) 165–170.
- [24] T. Ozawa, Y. Miura, J.I. Ueda, *Free Radic. Biol. Med.* 20 (1996) 837–841.
- [25] R. Nakamura, Y. Nakato, *J. Am. Chem. Soc.* 126 (2004) 1290–1298.
- [26] R. Nakamura, T. Okamura, N. Ohashi, A. Imanishi, Y. Nakato, Y. Nakato, *J. Am. Chem. Soc.* 127 (2005) 12975–12983.
- [27] S. Sroiraya, W. Triampo, N. Morales, D. Triampo, *J. Ceram. Process. Res.* 9 (2008) 146–154.
- [28] C. Jones, *Applications of Hydrogen Peroxide and Derivatives*, R. Soc. Chem. (1999) 264.